Fluorescent Indolo[3,2-*a*]phenazines against *Toxoplasma gondii*: Concise Synthesis by Gold-Catalyzed Cycloisomerization with 1,2-Silyl Migration and *ipso*-Iodination Suzuki Sequence

Franziska K. Merkt,[a] Flaminia Mazzone,[b] Shabnam Shaneh Sazzadeh,[b] Lorand Bonda,[a] Larissa K. E. Hinz,[a] Irina Gruber,[c] Karin Buchholz,[b] Christoph Janiak,[c] Klaus Pfeffer,[b] and Thomas J. J. Müller*[a]

Dedicated to Prof. Dr. Ari M. P. Koskinen on the occasion of his 65th birthday

Abstract: A gold-catalyzed cycloisomerization of 2-indolyl-3-[(trimethylsilyl)ethynyl)]quinoxalines with concomitant 1,2-silyl shift forms 6-(trimethylsilyl)indolo[3,2-*a*]phenazines in moderate to excellent yield. These silylated heterocycles are readily transformed into 6-aryl-indolo[3,2-*a*]phenazines in moderate to good yield by one-pot *ipso*-iodination Suzuki coupling. The title compounds represent a novel type of tunable luminophore. Structure-property relationships for 6-aryl-indolo[3,2-*a*]phenazines obtained from Hammett correlations with σ_{p+} substituent parameters indicate that emission maxima, Stokes shifts, and fluorescence quantum yields can be fine-tuned by the remote *para*-aryl substituent. Furthermore, indolo[3,2-*a*]phenazines were found to exhibit interesting activities against medically relevant pathogens such as the Apicomplexa parasite *Toxoplasma gondii* with an IC_{50} of up to 0.67 ± 0.13 μM. Thus, these compounds are promising candidates for novel anti-parasitic therapies.

Introduction

Indolo[3,2-*a*]phenazine (**1**; Figure 1) represents a highly interesting fused pentaheterocyclic structure consisting of the angular anellation of electron-rich indole to the electron-poor phenazine, which has not been deeply explored in its properties to date. By in silico docking studies indolo[3,2-*a*]phenazine **2** was identified as a novel inhibitor of NAD(P)H quinone oxidoreductase,[1] due to strong interaction with gene NQO1, which can be responsible for the overexpression of tumor cells and inhibitors of this enzyme have been proposed as potent anticancer agents.[2] The pentacyclic structure with donor-acceptor separation additionally resembles to that of berberine hemisulfate (**3**), belonging to the protoberberine group of benzylisoquinoline alkaloids with considerable pharmacological applications in many different indications.[3] In particular, berberine and derivatives are considered as alternative treatment options against the parasite *Toxoplasma gondii*.[4]

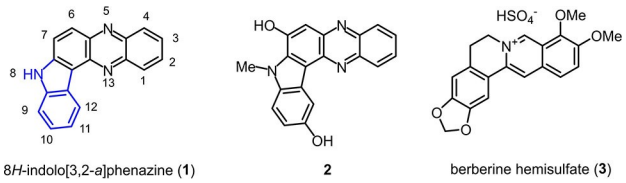

Figure 1. 8*H*-indolo[3,2-*a*]phenazine (**1**), a potentially potent anticancer agent **2** (from in silico docking studies), and berberine hemisulfate (**3**).

T. gondii is an obligate intracellular parasite belonging to the phylum Apicomplexa, which includes known human pathogens such as the agent of tropical malaria *Plasmodium falciparum*, with which it shares significant biological similarities.[5] *T. gondii* is the causative agent of toxoplasmosis and is considered one of the world's most successful parasites due its ability to infect a wide range of warm-blooded vertebrate intermediate hosts, including humans.[6] It is estimated that one-third of the human population is chronically

[a] Dr. F. K. Merkt, L. Bonda, L. K. E. Hinz, Prof. Dr. T. J. J. Müller
Institut für Organische Chemie und Makromolekulare Chemie
Heinrich-Heine-Universität Düsseldorf
Universitätsstraße 1, 40225 Düsseldorf (Germany)
E-mail: ThomasJJ.Mueller@hhu.de

[b] F. Mazzone, Dr. S. S. Sazzadeh, K. Buchholz, Prof. Dr. K. Pfeffer
Institut für Medizinische Mikrobiologie und Krankenhaushygiene
Heinrich-Heine-Universität Düsseldorf
Universitätsstraße 1, 40225 Düsseldorf (Germany)

[c] Dr. I. Gruber, Prof. Dr. C. Janiak
Institut für Anorganische Chemie und Strukturchemie
Heinrich-Heine-Universität Düsseldorf
Universitätsstraße 1, 40225 Düsseldorf (Germany)

Supporting information for this article is available on the WWW under https://doi.org/10.1002/chem.202101391

infected with *T. gondii*[7] which is acquired mainly through two ways: by ingesting tissue cysts from raw or undercooked meat or by ingesting oocysts shed from feline hosts (the definitive hosts) with contaminated food or water.[8] In immunocompetent individuals, the infection with *T. gondii* is usually inapparent with minor or no symptoms, but it can be fatal in immunocompromised individuals due to reactivation of latent infections.[9] In addition, early maternal infection during pregnancy may result in fetal death, spontaneous abortion, and birth defects.[10] Treatments of acute toxoplasmosis are largely limited to antifolate therapy, based on the combination of pyrimethamine and sulfadiazine supplemented with folic acid. As the second-line treatments, the antibiotics co-trimoxazole and clindamycin are used.[11] These regimens have high rates of toxic side effects leading to discontinuation of therapy. Thus, there is need to develop well-tolerated and less or nontoxic treatments options to improve the care of patients with toxoplasmosis.[12]

While phenazines have found entry in various dyes, such as *induline*,[13] *neutral red*,[14] or *safranin T*,[13] their indolo-fused analogues have remained unknown as chromophores. In synthetic chemistry only very few syntheses have been reported so far (Scheme 1).

While the parent system **1** was already assessed in 1954 by Teuber and Staiger by cyclocondensation of 3*H*-carbazol-3,4(9*H*)-dione and *ortho*-phenylene diamine (Scheme 1A),[15] similarly to the Hinsberg synthesis of quinoxaline, the title compounds remained unexplored. Only a few years ago, the groups of Kurth and Haddadin presented an acid-catalyzed Friedländer synthesis with 2,3-dihydro-1*H*-cyclopenta[*b*]quinoxalinen-1-one and 2-aminobenzaldehyde furnishing a mixture of 8*H*-indolo[3,2-*a*]phenazine and quinolin[2,3-*c*]cyclopentadienone[2,3-*b*]quinoxaline, however, with 8*H*-indolo[3,2-*a*]phenazine as the minor product.[16] Recently, Kumar and Pal reported a general synthesis of indolo[3,2-*a*]phenazines in good yield by trifluoroacetic acid catalyzed cycloisomerization of indole-substituted 3-ethynylquinoxalines (Scheme 1B).[17] Interestingly, gold-catalyzed cycloisomerization of 3-ethynylquinoxalines was not reported in this study. Based upon our long standing experience in consecutive multicomponent syntheses of quinoxalines[18] and their photophysical properties,[18b–f,19] we envisioned that our multicomponent access to 3-ethynylquinoxalines provides an excellent basis for developing syntheses of specifically substituted 8*H*-indolo[3,2-*a*]phenazines in the sense of diversity-oriented level-2 transformations (Scheme 1C). Here, we report on a novel synthesis of 6-trimethylsilyl 8*H*-indolo[3,2-*a*]phenazines, their one-pot *ipso*-iodination-Suzuki coupling to 6-arylsubstituted 8*H*-indolo[3,2-*a*]phenazines, the photophysical characteristics of these novel systems as well as the biological testing of their activity against the parasite *T. gondii*.

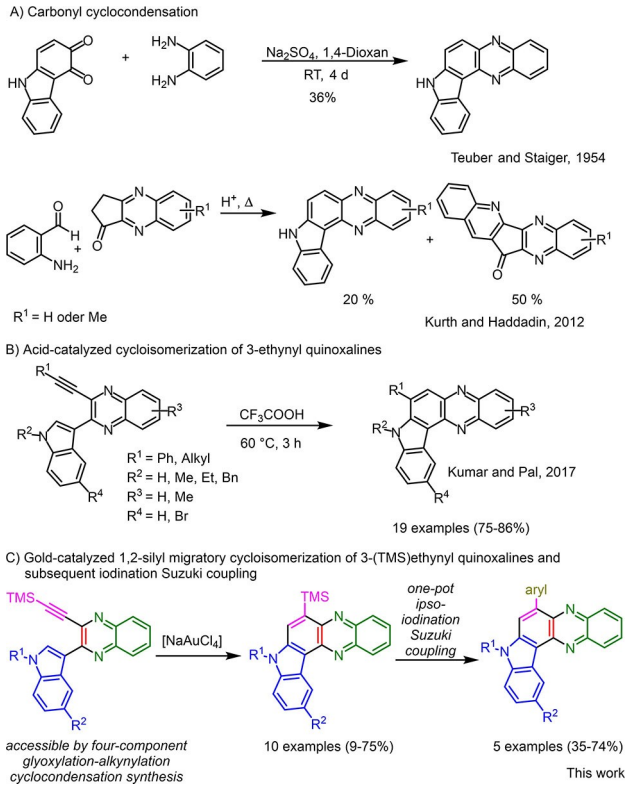

Scheme 1. Synthetic approaches to 8*H*-indolo[3,2-*a*]phenazines.

Results and Discussion

Synthesis and structure

In past years, we have disclosed several consecutive multicomponent syntheses of various 2-indolyl-3-[(trimethylsilyl)ethynyl)]quinoxalines based upon glyoxylation-alkynylation-cyclocondensation (GACC) or activation-alkynylation-cyclocondensation (AACC) strategies furnishing 3-ethynyl quinoxalines as key intermediates.[18b–f] To quickly provide suitable substrates for testing the cycloisomerization of 3-ethynyl quinoxalines to 8*H*-indolo[3,2-*a*]phenazines, we chose the GACC synthesis starting from various indoles (**4**), oxalylchloride (**5**), (trimethylsilyl)acetylene (**6**), and *ortho*-phenylenediamine (**7**) to give 2-indolyl-3-[(trimethylsilyl)ethynyl)]-quinoxalines **8** in good to excellent yield (Scheme 2).

With 3-[(trimethylsilyl)ethynyl)]quinoxaline **8a** and its desilyated congener 3-(ethynyl)quinoxaline **8l** in hand (compound **8l** was prepared from compound **8a** by desilylation with KF in MeOH[18e]), we set out with two model reactions to screen conditions for the cycloisomerization to indolo[3,2-*a*]phenazines **9a** and **9l** (Scheme 3, for details, see the Supporting Information, Chapter 3, and Table S2). Among several carbophilic Lewis acids[20] only auric chloride ($AuCl_3$) cycloisomerizes alkyne **8l** to indolo[3,2-*a*]phenazine **9l** in moderate yield and $NaAuCl_4$ proves to be an inefficient catalyst for this substrate. However, while for alkyne **8a** Kumar's and Pal's conditions (excess of trifluoroacetic acid)[17] failed $NaAuCl_4$ turns out to be the catalyst of choice in toluene at 80 °C for cycloisomerizing compound **8a** to indolo[3,2-*a*]phenazine **9a**. Most interestingly the cycloisomerization proceeds with concomitant 1,2-silyl migration.

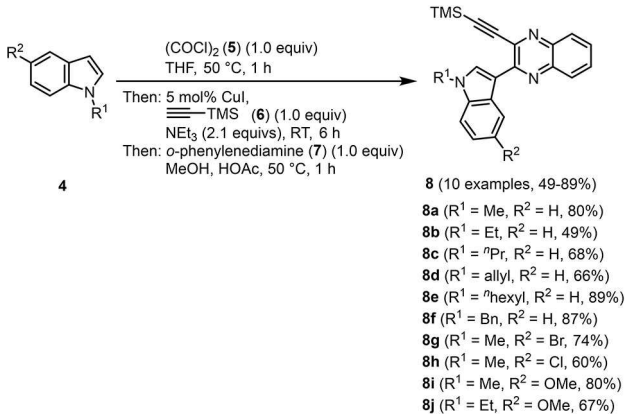

Scheme 2. Consecutive four-component GACC synthesis of 2-indolyl-3-[(trimethylsilyl)ethynyl)]quinoxalines **8**.

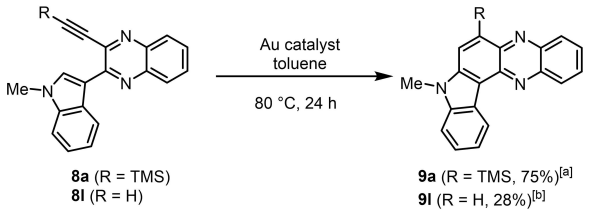

Scheme 3. Test reaction for the cycloisomerization of compounds **8** to indolo[3,2-*a*]phenazines **9**. [a] 2 mol% $NaAuCl_4$; [b] 40 mol% $AuCl_3$.

The structures of the cycloisomerization products **9a** and **9k** are unambiguously supported by extensive NMR spectroscopy, and in addition the structure of indolo[3,2-*a*]phenazine **9a** was corroborated by an X-ray structure analysis (Figure 2).[21] The crystal structure additionally reveals π-π interactions.

The gold-catalyzed cycloisomerization of 3-[(trimethylsilyl)-ethynyl)]quinoxaline **8a** to furnish 8-methyl-6-(trimethylsilyl)-indolo[3,2-*a*]phenazine (**9a**) represents a 6-*endo-dig* cyclization of the indole moiety and the alkyne unit with concomitant 1,2-silyl migration. Group IV elements (carbon, silicon, germanium, and tin) might undergo 1,2-migrations in alkyne-vinylidene isomerization via a gold carbenoid[22] and with related 1,2-silyl-shifts of the vinyl-gold species[23] as intermediates. To gain some mechanistic insight, we treated a selectively deuterated substrate **8k** with 100% deuterium at position 2 of the indole part to give 53% of indolo[3,2-*a*]phenazine **9k** containing 70% deuterium at position 7 (Scheme 4). Obviously not only the silyl group undergoes a 1,2-silyl shift but also 1,2-hydride shift occurs in the sequence. This observation can be rationalized by two alternative scenarios. Assuming an Au carbenoid pathway (Scheme 4, pathway A) after coordination of the catalyst to the triple bond the 1,2-silyl shift generates gold vinylidene complex **10a**, which cyclizes to give carbenoid **11a** according to Gevorgyan's rationale.[22b] The subsequent 1,2-H(D) shift furnishes the zwitterion **12a** that produces the product upon deauration. Alternatively, pathway B (Scheme 4) commences with the intramolecular nucleophilic attack of the indole moiety at the Au-activated triple bond to give the cyclized zwitterionic vinyl-gold intermediate **13a** according to Fürstner's rationale.[23] The subsequent 1,2-H(D) shift first generates the β-silyl stabilized indoliminium intermediate **14a**, which then undergoes a 1,2-silyl shift maintaining the β-silyl cation stabilization in intermediate **15a**. Finally, deauration closes the catalytic

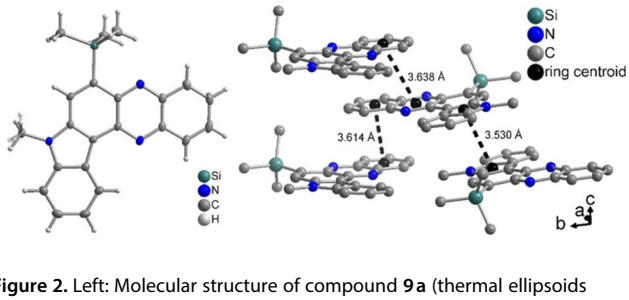

Figure 2. Left: Molecular structure of compound **9a** (thermal ellipsoids shown at the 50% probability level). Right: Section of the packing diagram of **9a** showing significant π-π interactions (labeled with their centroid–centroid distances; H atoms omitted for clarity). For further details, see Section 13 in the Supporting Information.

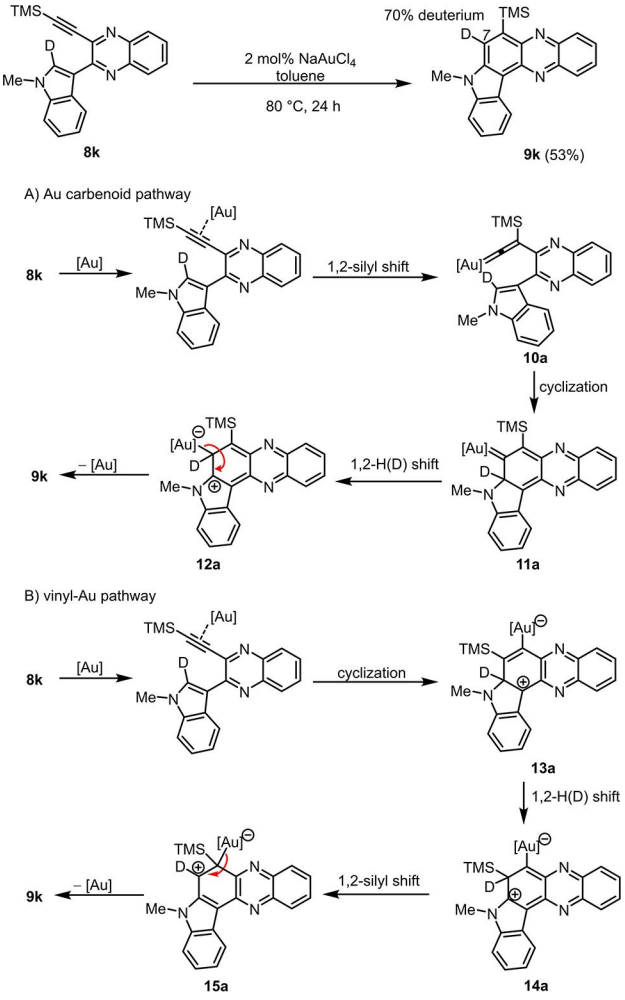

Scheme 4. Cycloisomerization with concomitant 1,2-silyl migration of selectively deuterated compound **8k** to give to give deuterated indolo[3,2-*a*]phenazine **9k** and two mechanistic scenarios.

cycle and liberates the cycloisomerization product **9k**. At this stage, both scenarios are in agreement of the result of the control experiment with the deuterated substrate **8k**.

With optimal conditions for the cycloisomerization of 3-[(trimethylsilyl)ethynyl)]quinoxalines **8** with concomitant 1,2-silylmigration in hand (see the Supporting Information, Chapter 3, and Table S2, entry 15) the stage was set for screening scope and limitation with respect to the substitution pattern on the indole moiety. Upon heating 3-[(trimethylsilyl)ethynyl)] quinoxalines **8** in toluene to 80 °C for 24 h in the presence of catalytic amounts of sodium tetrachloroaurate various indolo [3,2-*a*]phenazines **9** were obtained in moderate to good yield (Scheme 5). The proposed structures were unambiguously supported by ^{1}H and ^{13}C NMR spectroscopy, mass spectrometry, IR spectroscopy, and combustion analysis. From the N-substitution pattern, it can be seen that increasing steric bulk (from Me over Et, Pr, allyl, and hexyl to benzyl) causes a significant decrease in yield. Substitution in position 11 of the indolo[3,2-*a*] phenazine allows access to the electronically diverse derivatives, that is, 11-halogen- or 11-methoxy-substituted molecules.

Silyl (hetero)arenes are perfectly suited for functionalization by *ipso*-substitution,[24] a particular case of electrophilic aromatic substitution operating by efficient stabilization of β-silyl cation σ-complex intermediates. This transformation was probed by converting compound **9a** into 6-iodo-indolo[3,2-*a*]phenazine **16** (Scheme 6), which could be favorably employed as a substrate in subsequent coupling reactions. The optimal conditions are the use of 1.7 equiv. of ICl in dichloromethane and after stirring at −78 °C for 5 min and at room temp for 30 min the 6-iodo-indolo[3,2-*a*]phenazine **16** was obtained after isolation in 76% yield (for details, see the Supporting Information, Chapters 5 and 6, Table S4).

For arylation of iodo indolo[3,2-*a*]phenazine **16** we selected the Suzuki coupling.[25] In a quick optimization study with *p*-methoxyphenylboronic acid (**17a**) as a coupling partner, optimal conditions were identified with potassium carbonate as a base in a 2:1 DMF/water mixture at 100 °C for 18.5 h giving 6-(*p*-anisyl)-8-methyl-indolo[3,2-*a*]phenazine (**18a**) after isolation by flash chromatography in 75% yield (Scheme 7, for details, see the Supporting Information, Chapter 7, Table S5, entry 3).

To establish a novel one-pot *ipso*-iodination-Suzuki synthesis of 6-(*p*-anisyl)-8-methyl-indolo[3,2-*a*]phenazine (**18a**) starting from indolo[3,2-*a*]phenazine **9a**, a ^{1}H NMR-based optimization study was launched (for details, see the Supporting Information Chapter 8, Table S6). It is noteworthy to mention that for the optimal conditions (see the Supporting Information, Table S6, entry 10) the yield of compound **18a** after chromatography with this novel one-pot sequence (72%) is considerably higher than the combined yield (57%) of stepwise *ipso*-iodination (76%, Scheme 6) and Suzuki coupling (75%, Scheme 7). Besides practicality, this also underlines the superiority, efficiency and efficacy of one-pot processes over stepwise transformations.

With these optimized conditions in hand the one-pot *ipso*-iodination-Suzuki coupling synthesis of 6-aryl-indolo[3,2-*a*] phenazines **18** was illustrated with indolo[3,2-*a*]phenazine **9a** and boronic acids/boroate **17** in seven examples to give the targeted products after chromatography in 35–74% yield (Scheme 8).

The proposed structures were unambiguously supported by ^{1}H and ^{13}C NMR spectroscopy, mass spectrometry, IR spectroscopy, and combustion analysis, and in addition the structure of 6-aryl-indolo[3,2-*a*]phenazine **18e** was corroborated by an X-ray structure analysis (Figure 3).[21] The structure elucidation of compound **18e** shows full planarity of the pentacyclic indolo [3,2-*a*]phenazine scaffold with a torsional angle of 54.3° of the *p*-cyanophenyl substituent with respect to the indolo[3,2-*a*] phenazine mean plane. The crystal structure additionally reveals distinct dipolar π-π interactions (as low as 3.38 Å).

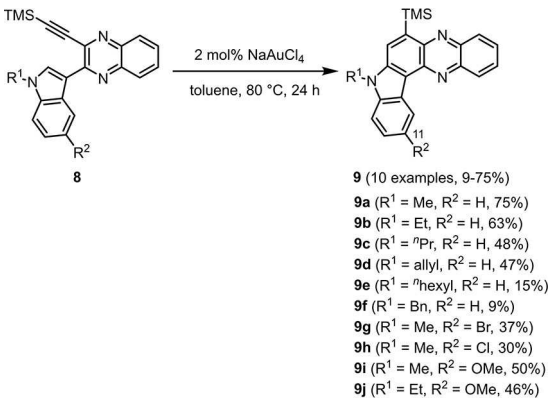

Scheme 5. Synthesis of indolo[3,2-*a*]phenazines **9** by gold-catalyzed cycloisomerization-1,2-silyl shift of 3-[(trimethylsilyl)ethynyl)]quinoxalines **8**.

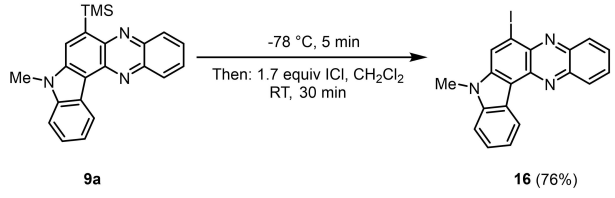

Scheme 6. Synthesis of 6-iodo-8-methyl-8*H*-indolo[3,2-*a*]phenazine (**16**) by electrophilic *ipso*-iodination with iodine monochloride.

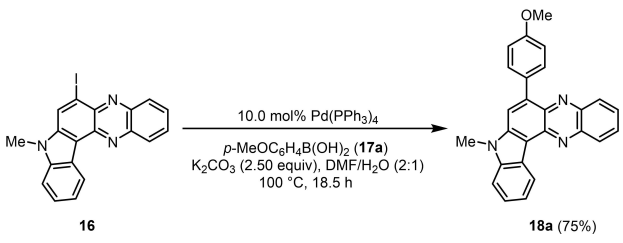

Scheme 7. Synthesis of compound **18a** by Suzuki coupling of 6-iodo-indolo [3,2-*a*]phenazine **16** with *p*-methoxyphenylboronic acid (**17a**).

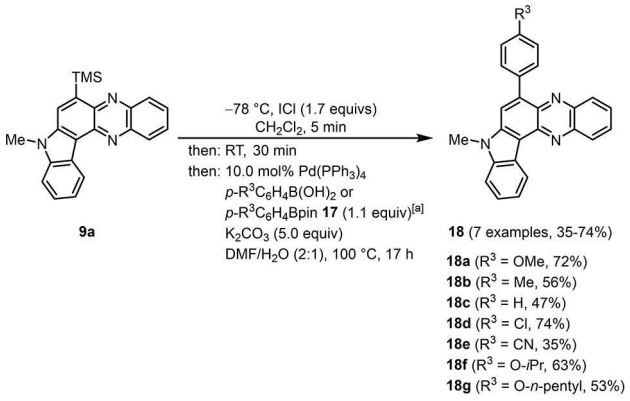

Scheme 8. One-pot *ipso*-iodination Suzuki coupling synthesis of 6-aryl-indolo[3,2-*a*]phenazines **18** from 6-(trimethylsilyl)indolo[3,2-*a*]phenazine **9a**.
[a] Boronate **17** was formed by bromine-lithium exchange and borylation, then the solution formed in situ was transferred to the iodo compound **16** formed in situ by syringe.

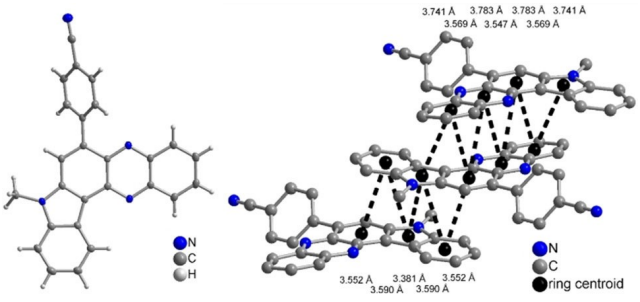

Figure 3. Left: Molecular structure of compound **18e** (thermal ellipsoids shown at the 50% probability level). Right: Section of the packing diagram of **18e** showing significant π-π interactions (with their centroid–centroid distances given; H atoms omitted for clarity). For further details, see Chapter 13 in the Supporting Information.

Photophysical properties and electronic structure of 6-substituted Indolo[3,2-*a*]phenazines

The luminescence of solutions of 6-substituted indolo[3,2-*a*]phenazines **9** and **18** in dichloromethane after excitation under a handheld UV lamp can be seen even by the naked eye (for a detailed analysis, see the Supporting Information, Chapter 11). The emission intensity of 6-(trimethylsilyl)indolo[3,2-*a*]phenazines **9** grows with the increasing electron-donor character of substituent R^3 to a maximum for the fluorescence quantum yield Φ_f of 28% (Table S8). The presence of two basic nitrogen atoms in 6-(trimethylsilyl)indolo[3,2-*a*]phenazine **9** suggests halochromicity of the underlying chromophore. Indeed, protonation of indolo[3,2-*a*]phenazine **9a** with trifluoroacetic acid (TFA) gives a pK_a of 5.60 for the protonated chromophore **9a-H$^+$**, that is, about four orders of magnitude less acidic than simple phenazine-H$^+$ ($pK_a = 1.2$).[26] Upon protonation the fluorescence signal is quenched (see the Supporting Information, Figure S57B).

As found for compounds **9**, 6-arylindolo[3,2-*a*]phenazines **18** display an increase of the fluorescence quantum yield Φ_f with increasing donor strength of substituent R^3 from 16% (R^3=CN) to 52% (R^3=OMe; see the Supporting Information, Table S9). Structure-property correlations based upon free energy linear relationships (LFER) with Hammett parameters σ^+ were unanimously found for absorption maxima $\lambda_{max,abs}$, emission maxima $\lambda_{max,em}$, Stokes shifts $\Delta\tilde{\nu}$ (see the Supporting Information, Figure S60A), and relative fluorescence quantum yields Φ_f (see the Supporting Information, Figure S60B). While only a minor polarity effect on the electronic ground state $\lambda_{max,abs}$ can be assigned from slope of the Hammett correlation, all effects reflecting the excited state ($\lambda_{max,em}$, $\Delta\tilde{\nu}$, Φ_f) strongly depend on stabilization of positive partial charges as supported by the σ_{p+} substituent parameter.

In addition, all compounds **18** are also luminescent in the solid state, however, with variable emission color (Figure 4). While compound **18a** (R^3=OMe) is yellow under the handheld UV-lamp, electron-deficient substituted **18e** (R^3=CN) is orange.

A deeper understanding of the electronic transitions in the absorption spectra of selected 6-aryl-8*H*-indolo[3,2-*a*]phenazines **18a**, **18c**, and **18e** was sought by calculating UV/Vis absorption spectra on the DFT level of theory using Gaussian09[27] with CAM–B3LYP[28] as a functional and the Pople 6-311+G(d,p) basis set.[29] Since the absorption spectra were recorded in dichloromethane solutions, the polarizable continuum model (PCM) with dichloromethane as a solvent was applied.[30]

The experimentally determined longest wavelength absorption bands are reasonably well reproduced by the TD-DFT calculations (see the Supporting Information, Table S10). As expected, the longest wavelength absorption bands of all three calculated 6-aryl-8*H*-indolo[3,2-*a*]phenazines originate from dominant contributions of HOMO–LUMO based transitions. In the HOMO of structures **18** the coefficient density is predominantly localized on the carbazole moiety of the indolo[3,2-*a*]phenazine, while the coefficient density in the LUMO almost exclusively is localized on the phenazine part (see the Supporting Information, Figure S61). This is in agreement with an angular charge transfer transition from donor (carbazole moiety) to acceptor (phenazine moiety).

Biological properties and activity against *T. gondii*

Indolo[3,2-*a*]phenazines are structurally related to the natural product berberine hemisulfate, which demonstrated anti-

Figure 4. Solid state fluorescence of 6-aryl-8*H*-indolo[3,2-*a*]phenazines **18a** (left) and **18e** (right; λ_{ex} = 365 nm).

toxoplasma activity.[4] Also in this study, an IC_{50} was determined for berberine hemisulfate (**3**) of 0.94 μM against *T. gondii* ME49 (Table 1, for experimental details, see the Supporting Information). The aim of this part of the study was to investigate the anti-toxoplasma activities of seven selected synthetic indolo [3,2-*a*]phenazines (**9a**, **18a**–**d**, **18f**–**g**) and to compare them with the anti-*T. gondii* activity of berberine hemisulfate. To achieve this aim, *T. gondii* proliferation assays were performed.

Table 1. *In vitro* activity of the selected synthetic indolo[3,2-*a*]phenazines **9** and **18** and berberine hemisulfate (**3**) against the *T. gondii* strain ME49.[a]

Compound[a]	IC50 ± SD [μM]	Compound[a]	IC50 ± SD [μM]
3	0.94 ± 0.48	**18c**	0.73 ± 0.27
9a	1.68 ± 0.88	**18d**	2.38 ± 0.86
18a	2.58 ± 1.68	**18f**	3.3 ± 2.29
18b	0.67 ± 0.13	**18g**	3.07 ± 1.75

[a] Toxoplasma proliferation assays were performed to investigate the activity of the selected synthetic indolo[3,2-*a*]phenazines against the *T. gondii* ME49 strain. Hs27 cells in a monolayer were cultured in 96-well plates and infected with *T. gondii* (2×10^4). Infected cells were treated with indolo[3,2-*a*]phenazines **9**, **18a**–**d**, **18f**–**g**, and berberine hemisulfate (**3**) at the concentration range of 0.15–20.00 μM at 37 °C for 48 h. Afterwards, the assays were labelled with ^{3}H–U (5mCi, diluted 1:30) at 37 °C for 28–30 h. Based on the incorporation of ^{3}H–U into the parasite nucleic acid, the parasite growth was quantified. As controls, uninfected Hs27 cells without treatment, IFNγ pre-stimulated infected cells and only *T. gondii* infected cells were used (Figure S63). Three independent assays, in duplicates, were performed. IC_{50} values and mean ± SD of each compound of the three independent experiments are shown.

All the tested compounds showed an anti-toxoplasma activity with an IC_{50} lower than 3.5 μM (Table 1 and Figure S63). The comparison with the IC_{50} value of berberine hemisulfate (**3**; 0.94 μM), demonstrated that **18b** and **18c** were slightly more effective inhibitors than berberine hemisulfate (**3**) with IC_{50} values 0.67 and 0.73 μM, respectively.

In order to evaluate whether the selected synthetic indolo [3,2-*a*]phenazines inhibit cell mitochondria of the host cell, MTT assays were performed. The synthetic indolo[3,2-*a*]phenazines **9** and **18** were, at the concentration range between 0.15-5.00 μM, not cytotoxic to Hs27 cells comparable to berberine hemisulfate (**3**). The synthetic indolo[3,2-*a*]phenazines **9**, **18a**–**d**, and **18f**–**g** showed moderate toxicity against Hs27 fibroblasts at concentrations starting at 10.00 μM (Figure 5). These results indicate that indolo[3,2-*a*]phenazines are effective inhibitors of *T. gondii* proliferation, and compounds **18b** and **18c** were found to be most effective.

With regard to the anti-toxoplasma activity of indolo[3,2-*a*] phenazines, compounds containing TMS-, phenyl, *p*-chlorophenyl, *p*-tolyl, *p*-methoxyphenyl, *p*-pentoxyphenyl and *p*-isopropyloxyphenyl moieties bound to the phenazine core-structure inhibited *T. gondii* (type II, strain ME49) very efficiently with $IC_{50} < 3.5$ μM (Table 1). Interestingly, the activity of berberine hemisulfate (**3**) in this study was very comparable to the previous report by Kryvogorsky et al.[4] using the RH *T. gondii* strain. Thus, promising leads of this study (**18b** and **18c**) are well suited for developing modified and even more active analogues in the future.

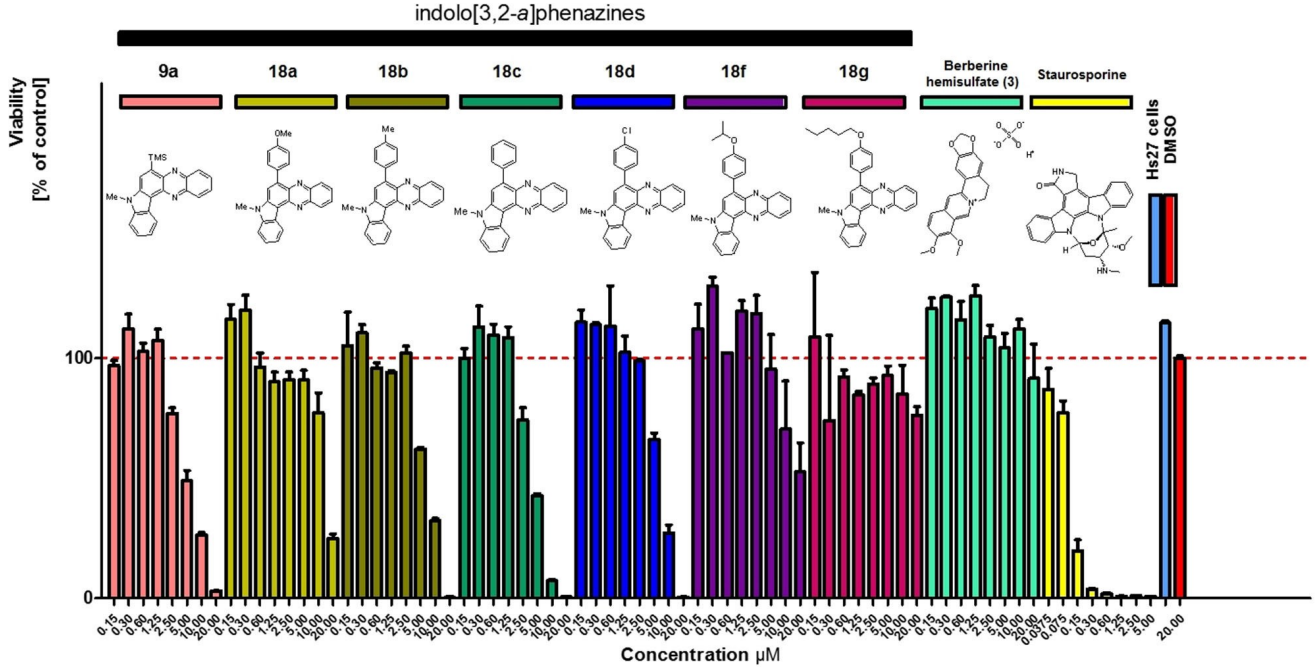

Figure 5. Effect of indolo[3,2-*a*]phenazines and **9** and **18** and berberine hemisulfate (**3**) on the metabolic activity of Hs27 cells. Hs27 cells were plated in 96-well plates and grown to confluence prior to incubation at 37 °C for 24 h with the selected synthetic indolo[3,2-*a*]phenazines and berberine hemisulfate at concentrations of 0.15–20.00 μM. The cultures were incubated with 10 μL of the 12 mM MTT stock solution for approximately 4 h. Afterwards, 100 μL of SDS dissolved in HCl was added to each well, and the plate was incubated again for 4 h at 37 °C. Finally, the absorbance was measured at 570 nm by spectrophotometry. Staurosporine (yellow) at concentrations of 0.0375–5.00 μL, Hs27 cells without treatment (blue) and DMSO (red) at the concentration of 20.00 μM were used as controls. Three independent assays were performed in duplicate; mean values ± SD are shown.

Conclusion

In summary, by gold-catalyzed cycloisomerization with a concomitant 1,2-silyl shift, 6-(trimethylsilyl)indolo[3,2-*a*]phenazines have been synthesized in moderate to excellent yield from 2-indolyl-3-[(trimethylsilyl)ethynyl)]quinoxalines, which were obtained by consecutive four-component synthesis. This novel type of indolo[3,2-*a*]phenazine is readily transformed in a one-pot *ipso*-iodination Suzuki coupling synthesis into 6-aryl-indolo[3,2-*a*]phenazines in moderate to good yield. Indolo[3,2-*a*]phenazines, as rigid pentaheterocyclic scaffolds consisting of a fused carbazole (donor) and phenazine (acceptor) moieties, represent an interesting novel type of luminophore that can be tuned in their emission characteristics, such as emission color and fluorescence quantum yield, by substituent decoration. Structure-property relationships were obtained for 6-aryl-indolo[3,2-*a*]phenazines from Hammett correlations with σ_{p+} substituent parameters, indicating that excited state properties, such as emission maxima, Stokes shifts and fluorescence quantum yields, in particular are affected and tunable by the remote *para*-aryl substituent. Furthermore, none of the synthetic indolo[3,2-*a*]phenazines showed relevant cytotoxicity against Hs27 cells over the concentration range 0.15–5.00 μM. Phenyl- and *p*-tolyl-substituted derivatives possess an intriguing Toxoplasma inhibitory effect with IC_{50} values lower than berberine hemisulfate and therefore do not have a relevant effect on the metabolic activity of Hs27 cells. This establishes the phenyl and toluene moieties connected to the phenazine core-structure as suitable substituents, with more attractive structure-activity properties against *T. gondii* than the other synthetic indolo[3,2-*a*]phenazines tested in this study. Therefore, the next step to be considered is the in vivo testing of the lead indolo[3,2-*a*]phenazines for toxicity and activity against *T. gondii* infections.

Acknowledgements

This work was supported by the Deutsche Forschungsgemeinschaft (GRK 2158, Mu 1088/9-1) and the Fonds der Chemischen Industrie. Open access funding enabled and organized by Projekt DEAL.

Conflict of Interest

The authors declare no conflict of interest.

Keywords: bioactivity · cycloisomerization · heterocycles · iodination · multicomponent reactions · *Toxoplasma gondii*

[1] K. A. Nolan, D. J. Timson, I. J. Stratforda, R. A. Bryce, *Bioorg. Med. Chem. Lett.* **2006**, *16*, 6246–6254.
[2] a) J. Bian, X. Qian, B. Deng, X. Xu, X. Guo, Y. Wang, X. Li, H. Sun, Q. You, X. Zhang, *RSC Adv.* **2015**, *5*, 49471–49479; b) K. A. Scott, J. Barnes, R. C. Whitehead, I. J. Stratford, K. A. Nolan, *Biochem. Pharmacol.* **2011**, *81*, 355–363.
[3] For lead reviews on the pharmacological profile and applications of berberine, see, e.g., a) K. Zou, Z. Li, Y. Zhang, H.-y. Zhang, B. Li, W.-l. Zhu, J.-y. Shi, Q. Jia, Y.-m. Li, *Acta Pharmacol. Sin.* **2017**, *38*, 157–167; b) M. Tillhon, L. M. G. Ortiz, P. Lombardi, A. I. Scovassi, *Biochem. Pharmacol.* **2012**, *84*, 1260–1267; c) J. Tang, Y. Feng, S. Tsao, N. Wang, R. Curtain, Y. Wang, *J. Ethnopharmacol.* **2009**, *126*, 5–17; d) M. Imanshahidi, H. Hosseinzadeh, *Phytother. Res.* **2008**, *22*, 999–1012.
[4] B. Krivogorsky, J. A. Pernat, K. A. Douglas, N. J. Czerniecki, P. Grundt, *Bioorg. Med. Chem. Lett.* **2012**, *22*, 2980–2982.
[5] I. Tardieux, R. Ménard, *Traffic* **2008**, *9*, 627–635.
[6] J. P. Webster, *Parasites Vectors* **2010**, *3*, 112.
[7] G. Pappas, N. Roussos, M. E. Falagas, *Int. J. Parasitol.* **2009**, *39*, 1385–1394.
[8] J. C. Sepúlveda-Arias, J. E. Gómez-Marin, B. Bobić, C. A. Naranjo-Galvis, O. Djurković-Djaković, *Travel. Med. Infect. Dis.* **2014**, *12*, 592–601.
[9] L. Machala, P. Kodym, M. Malý, M. Geleneky, O. Beran, D. Jilich, *Epidemiol. Mikrobiol. Imunol.* **2015**, *64*, 59–65.
[10] A. Elbez-Rubinstein, D. Ajzenberg, M.-L. Dardé, R. Cohen, A. Dumètre, H. Yera, E. Gondon, J.-C. Janaud, P. Thulliez, *J. Infect. Dis.* **2009**, *199*, 280–285.
[11] H. B. Fung, H. L. Kirschenbaum, *Clin. Ther.* **1996**, *18*, 1037–1056.
[12] P. Alday, J. Doggett, *Drug Des. Dev. Ther.* **2017**, *11*, 273–293.
[13] H. Berneth, *Azine Dyes, Ullmann's Encyclopedia of Industrial Chemistry, Vol. 4*, Wiley-VCH, Weinheim, **2012**, pp 475–514.
[14] G. Repetto, A. del Peso, J. L. Zurita, *Nat. Protoc.* **2008**, *3*, 1125–1131.
[15] H.-J. Teuber, G. Staiger, *Chem. Ber.* **1954**, *87*, 1251–1253.
[16] T. A. Shoker, K. I. Ghattass, J. C. Fettinger, M. J. Kurth, M. J. Haddadin, *Org. Lett.* **2012**, *14*, 3704–3707.
[17] K. S. Kumar, B. Bhaskar, M. S. Ramulu, N. P. Kumar, M. A. Ashfaq, M. Pal, *Org. Biomol. Chem.* **2017**, *15*, 82–87.
[18] a) P. Niesobski, I. Santana Martínez, S. Kustosz, T. J. J. Müller, *Eur. J. Org. Chem.* **2019**, 5214–5218; b) F. K. Merkt, K. Pieper, M. Klopotowski, C. Janiak, T. J. J. Müller, *Chem. Eur. J.* **2019**, *25*, 9447–9455; c) F. K. Merkt, S. P. Höwedes, C. F. Gers-Panther, I. Gruber, C. Janiak, T. J. J. Müller, *Chem. Eur. J.* **2018**, *24*, 8114–8125; d) F. K. Merkt, T. J. J. Müller, *Sci. China Chem.* **2018**, *61*, 909–924; e) C. F. Gers-Panther, H. Fischer, J. Nordmann, T. Seiler, T. Behnke, C. Würth, W. Frank, U. Resch-Genger, T. J. J. Müller, *J. Org. Chem.* **2017**, *82*, 567–578; f) C. F. Gers, J. Nordmann, C. Kumru, W. Frank, T. J. J. Müller, *J. Org. Chem.* **2014**, *79*, 3296–3310.
[19] a) M. M. Lindic, M. Zajonz, C. Gers-Panther, T. J. J. Müller, M. Schmitt, *Spectrochim. Acta Part A* **2020**, *228*, 117574; b) N. Nirmalananthan, T. Behnke, K. Hoffmann, D. Kage, C. F. Gers-Panther, W. Frank, T. J. J. Müller, U. Resch-Genger, *J. Phys. Chem. C* **2018**, *122*, 11119–11127.
[20] For reviews on π-Lewis acids, see e.g. a) A. Fürstner, P. W. Davies, *Angew. Chem. Int. Ed.* **2007**, *46*, 3410–3449; *Angew. Chem.* **2007**, *119*, 3478–3519; *Angew. Chem.* **2007**, *119*, 3478–3519; *Angew. Chem. Int. Ed.* **2007**, *46*, 3410–3449; b) A. S. K. Hashmi, *Chem. Rev.* **2007**, *107*, 3180–3211; c) D. J. Gorin, D. Toste, *Nature* **2007**, *446*, 395–403.
[21] Deposition numbers 2061296 (for **9a**) and CCDC-2061297 (for **18e**) contain the supplementary crystallographic data for this paper. These data are provided free of charge by the joint Cambridge Crystallographic Data Centre and Fachinformationszentrum Karlsruhe Access Structures service.
[22] a) I. V. Seregin, V. Gevorgyan, *J. Am. Chem. Soc.* **2006**, *128*, 12050–12051; b) I. Nakamura, T. Sato, M. Terada, Y. Yamamoto, *Org. Lett.* **2007**, *9*, 4081–4083; c) Y. Xia, A. S. Dudnik, Y. Li, V. Gevorgyan, *Org. Lett.* **2010**, *12*, 5538–5541.
[23] V. Mamane, P. Hannen, A. Fürstner, *Chem. Eur. J.* **2004**, *10*, 4556–4575.
[24] For selected reviews, see e.g. a) S. M. Bonesi, M. Fagnoni, *Chem. Eur. J.* **2010**, *16*, 13572–13589; b) B. A. Keay, *Chem. Soc. Rev.* **1999**, *28*, 209–215; c) T. H. Chan, I. Fleming, *Synthesis* **1969**, 761–786; d) B. Bennetau, J. Dunogues, *Synlett* **1993**, 171–176.
[25] For selected reviews on Suzuki coupling, see, e.g., a) A. Suzuki, *Angew. Chem. Int. Ed.* **2011**, *50*, 6722–6737; *Angew. Chem.* **2011**, *123*, 6854–6869; *Angew. Chem.* **2011**, *123*, 6854–6869; *Angew. Chem. Int. Ed.* **2011**, *50*, 6722–6737; b) H. Doucet, *Eur. J. Org. Chem.* **2008**, 2013–2030; c) N. Miyaura, A. Suzuki, *Chem. Rev.* **1995**, *95*, 2457–2483.
[26] U. Urleb, S. Gobec, *Product Class 16: Phenazines, Science of Synthesis, Vol. 16*, Thieme, Stuttgart, **2004**, pp 913–943.
[27] M. J. Frisch, G. W. Trucks, H. B. Schlegel, G. E. Scuseria, M. A. Robb, J. R. Cheeseman, G. Scalmani, V. Barone, B. Mennucci, G. A. Petersson, H. Nakatsuji, M. Caricato, X. Li, H. P. Hratchian, A. F. Izmaylov, J. Bloino, G. Zheng, J. L. Sonnenberg, M. Hada, M. Ehara, K. Toyota, R. Fukuda, J. Hasegawa, M. Ishida, T. Nakajima, Y. Honda, O. Kitao, H. Nakai, T. Vreven, J. A. Montgomery, Jr., J. E. Peralta, F. Ogliaro, M. Bearpark, J. J. Heyd, E.

Brothers, K. N. Kudin, V. N. Staroverov, R. Kobayashi, J. Normand, K. Raghavachari, A. Rendell, J. C. Burant, S. S. Iyengar, J. Tomasi, M. Cossi, N. Rega, J. M. Millam, M. Klene, J. E. Knox, J. B. Cross, V. Bakken, C. Adamo, J. Jaramillo, R. Gomperts, R. E. Stratmann, O. Yazyev, A. J. Austin, R. Cammi, C. Pomelli, J. W. Ochterski, R. L. Martin, K. Morokuma, V. G. Zakrzewski, G. A. Voth, P. Salvador, J. J. Dannenberg, S. Dapprich, A. D. Daniels, O. Farkas, J. B. Foresman, J. V. Ortiz, J. Cioslowski, D. J. Fox, *Gaussian 09 (Revision A.02)* Gaussian, Inc., Wallingford CT, **2009**.

[28] a) C. Lee, W. Yang, R. G. Parr, *Phys. Rev. B* **1988**, *37*, 785–789; b) A. D. Becke, *J. Chem. Phys.* **1993**, *98*, 1372–1377; c) A. D. Becke, *J. Chem. Phys.* **1993**, *98*, 5648–5652; d) K. Kim, K. D. Jordan, *J. Phys. Chem.* **1994**, *98*, 10089–10094; e) P. J. Stephens, F. J. Devlin, C. F. Chabalowski, M. J. Frisch, *J. Phys. Chem.* **1994**, *98*, 11623–11627.

[29] R. Krishnan, J. S. Binkley, R. Seeger, J. A. Pople, *J. Chem. Phys.* **1980**, *72*, 650–654.

[30] G. Scalmani, M. J. Frisch, *J. Chem. Phys.* **2010**, *132*, 114110.

Manuscript received: April 18, 2021
Accepted manuscript online: April 21, 2021
Version of record online: May 27, 2021